Experimental Study on the Effects of Friction Stir Spot Welding Process Parameters on AL2024T3 Joint Strength

Majid Farhang
School of Mechanical Engineering,
College of Engineering, University of Tehran, Iran.
E-mail: m_farhang@ut.ac.ir

Mohammadreza Farahani*
School of Mechanical Engineering,
College of Engineering, University of Tehran, Iran.
E-mail: mrfarahani@ut.ac.ir
*Corresponding author

Moein Enami
School of Mechanical Engineering,
College of Engineering, University of Tehran, Iran.
E-mail: Moein_enami@ alumni.ut.ac.ir

Received: 26 April 2021, Revised: 17 August 2021, Accepted: 26 August 2021

Abstract: In this study, effects of process parameters of Friction Stir Spot Welding were investigated on Al2024T3 which has poor weldability. Several spot welds were performed by the FSSW process on the 2mm aluminium sheets. The effects of main process parameters such as tool Rotational Speed (RS), Normal Plunge Depth (NPD), and Dwell Time (DT) on the joint strength were investigated. By increasing the tool rotational speed, the joint strength increased, consequently. The mean failure load improved 52% when the tool rotational speed increased from 800 rpm to 1120 rpm, whereas increasing the rotational speed from 1120 to 1600 did not have significant effect on the failure load. The results showed, increasing the normal plunge depth from 1.5 to 1.75 millimetre led to an increase in the failure load of spot welds by about 1.62 times. Also, the 3 seconds dwell time showed higher failure load compared to 2 and 5 seconds dwell time.

Keywords: Aluminium 2024T3, Dwell Time, Failure Load, Friction Stir Spot Welding, Normal Plunge Depth, Rotational Speed

How to cite this paper: Majid Farhang, Mohammadreza Farahani, and Moein Enami, "Experimental Study on the Effects of Friction Stir Spot Welding Process Parameters on AL2024T3 Joint Strength", Int J of Advanced Design and Manufacturing Technology, Vol. 14/No. 4, 2021, pp. 105-112.
DOI: 10.30495/admt.2021.1922979.1280

Biographical notes: Majid Farhang received his BSc and MSc degree in Islamic Azad University and University of Tehran in 2012 and 2015, respectively. His research topics are residual stress analysis, and welding & joining. **Mohammadreza Farahani** received his PhD in Mechanical Engineering from Amir Kabir University of Technology where he was engaged in research in the field of residual stresses and welding technology and nondestructive testing in 2010. He is currently an Associate Professor in school of Mechanical Engineering at University of Tehran. His research interests include Nondestructive evaluation, welding, and adhesive joints. **Moein Enami** received his BSc and MSc degree in Islamic Azad University and University of Tehran in 2013 and 2016, respectively. His research topics are Material characterization and Advanced joining methods.

1 INTRODUCTION

Nowadays, light metals such as aluminium alloys are extensively used in various industries including the automotive and aerospace industries [1-3]. Resistance Spot Welding (RSW), laser spot welding, bolting and riveting methods were increasingly used for assembling the aluminium parts. For this reasons, a new spot welding process was developed for joining aluminium components [4]. This process is a continuation of the method developed in 1991 at the Welding Institute (TWI) in the United Kingdom for welding aluminium alloys [5-6]. This method was rapidly used in numerous industries alongside the traditional welding methods. The reasons for rapid development, particularly in welding of aluminium alloys, include the unique mechanical properties of the welded joint due to elimination of the defects resulting from melting including hot cracking, porosity, and entrapment of surface oxides [7]. Further these joints have lower residual stresses than arc welding methods [5], [8]. Therefore, there is no need for stress relief in the friction stir welding process [9-10].
As seen in “Fig. 1” , the FSSW process includes three steps: tool plunging, stirring of welded materials, and tool retracting [4], [11].

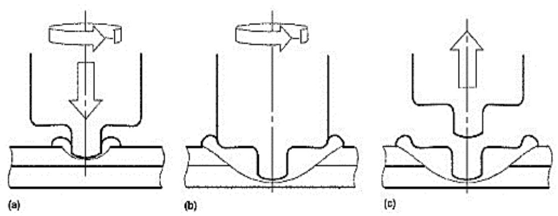

Fig. 1 Different steps of the FSSW process: (a): Plunging, (b): Stirring, and (c): Retracting [23].

The FSW method can also be used for joining zinc components and is widely used for joining 2xxx and 7xxx alloys that are difficult to make spot welds by conventional fusion welding methods [12-14]. The main process parameters by which the welded joints failure load can be determined, include rotational speed (RS), normal plunge depth (NPD), and dwell time (DT) of the tool [15-16]. Rotational speed of the tool has the most significant effect on generating the heat due to friction and mixing of materials. Increasing the rotational speed would increase the strain rate [17]. Kartikian et al. [18] and Arul et al. [19] evaluated FSSW processes with the tool covering the rotational speed ranges of 600-1800 rpm and 1500-3000 rpm, respectively. Applying an inadequate plunge depth might lead to cracks propagation as well as other defects [20]. Shen et al. [21] examined the effect of rotational speed and dwell time on the welding of the heat-treated alloy 7075, and argued that due to the existence of sediments in the microstructure, both these parameters affected the failure load and hardness of the spot welded joint. They also reported the more significant effect of tool rotational speed on the failure load of welded joint than the dwell time [21-22].
In this study, the effect of friction stir spot welding process parameters including rotational speed, dwell time, and normal plunge depth on the failure load of the 2024T3 aluminium alloy joints was investigated and the effect of these variables and their interactions were examined. This paper was conducted with the objective of reaching high fracture strength by means of reinforcing additives in Aluminium joints.

2 MATERIALS AND METHODS

2.1. Material

2-millimeter-thick sheets of 2024T3 aluminium alloy were used for the study. Table 1 and Table 2 show the chemical and mechanical properties of the aluminium alloy, respectively.

Table 1 Chemical composition of 2024T3 Al alloy

Element	Si	Zn	Fe	Cu	Mn	Mg
)%Weight (	0.5	0.25	0.5	3.9	0.7	1.5

Table 2 Mechanical properties of 2024T3 Al alloy

Ultimate tensile strength (MPa)	Yield strength(MPa)	Elongation
405	270	%14

The specimens were cut by 25x110 millimetre dimensions and used in the experiments. Prior to the welding process, the oxide layers on both sides of the specimen were cleaned by using fine sandpapers and acetone. Figure 2 shows a schematic of the two specimens obtained for the spot weld process.

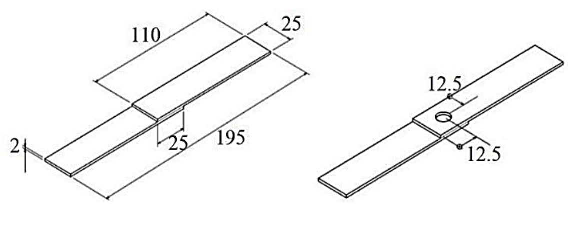

Fig. 2 Geometrical dimension and Position of spot weld on the samples (millimetre).

2.2. Friction Stir Spot Welding Process

The tool pin causes a material disturbance (stir) in the nugget zone. Different geometries of Friction stir spot welding tool have been performed in various researches [24-26]. Billichi et al. [27] compared the failure load of the FSSW joints by using cylindrical, truncated cone, threaded cylindrical, square, triangular, and hexagonal pin geometries. They concluded that at equal plunge depths, the cylindrical pin produced the highest joint failure load [27]. According to the study that used cylindrical pin, the pin length in the FSW method is selected based on the thickness of the sheets to be joined. Tozaki et al. [28] argued that the joint failure load increases with increasing the pin length (at maximum plunge depths upper than one fourth thickness of the bottom sheet). In addition, Bakavous et al. [29-30] reported that the best normal plunge depth for the pin is upper than 20 up to 25 percent of the lower sheet thickness.

The geometry of tool shoulder used in the FSSW method significantly influences the heat distribution during welding and provides the required compressive forces to perform the welded joint [31-32]. Also, the tool geometry conducts material plasticization around the pin, material flow within the welding zone and weld geometry [33]. Tool shoulder diameter also affects the heat generated during the welding process, tool rotational speed, axial force, and the volume of the welded zone [33-34]. Badarinarian et al. [35] studied three different geometries of the tool shoulder in the FSSW method. They investigated mechanical properties of the spot welded joints produced by three convex, flat, and concave tool shoulders. They proved that the failure load of the joint was improved by 15% when a concave tool shoulder was used as compared to flat and convex geometries [35].

According to the researches [35-37], the tool used in this investigation was manufactured by AISI H13 steel and had 5-millimetre pin diameter, 2.2-millimetre pin length, 14-millimetre tool shoulder and 10-degree concavity angle of the tool shoulder. The tool was hardened to increase its surface hardness up to 55 HRC to achieve required strength and endurance. Figure 3 shows the welding tool used in this study.

Fig. 3 FSSW tool used in the study.

A vertical milling machine with a semi-automatic controller was used for welding. The specimens were positioned in the supporting fixture in a way to prevent from undesirable displacement during welding. Figure 4 shows the fixture mounted on the milling machine table.

Fig. 4 The FSSW fixture on the milling machine table.

In the following, the welding process parameters were tested according to the designed experiments. The full factorial experiment design method with 18 tests was implemented. Table 3 shows the parameters variation ranges performed in this study. The normal plunge depth parameter (NPD) was defined by tool plunge depth divided by sheet thickness in the FSSW process.

Table 3 Mechanical properties of 2024T3 Al alloy

Dwell Time (DT)(s)			Rotational speed (RS)(rmp)			Normal Plunge Depth (NPD)(mm)	
2	3	5	800	1120	1600	1.5	1.75

The tension test was conducted on these specimens to examine the failure load of spot welds. A 30 ton SHIJIN 300E Class 1 Machine ("Fig. 5") was used for conducting the tension tests. The tests were conducted based on the JIS Z 3136: 1999 requirements at ambient temperature with speed of 1 mm/min. Tension was applied in the longitudinal direction of the test specimen.

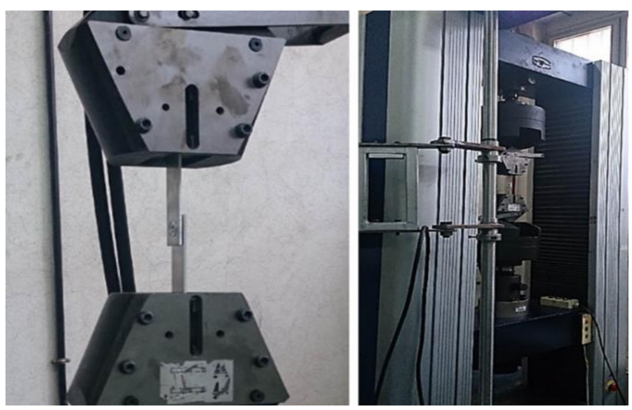

Fig. 5 Tensile test and sample placement at the machine.

3 RESULTS AND DISCUSSION

The specimens were prepared according to the process parameters which are specified as welding process parameters in "Table 3". Then the uniaxial tension tests were conducted. The failure load of FSSW joints were performed according to the design table.
To conduct better analysis of the process variables effects, the failure load of specimens obtained by tensile tests were initially examined. The interaction effects between the process parameters was studied in following sections.

3.1 Effect of Normal Plunge Depth on Failure Load

Normal plunge depth determines the contact conditions between the tool shoulder and the welding area. The spot welds failure load obtained in the tension test for the specimens are given in "Fig. 6".

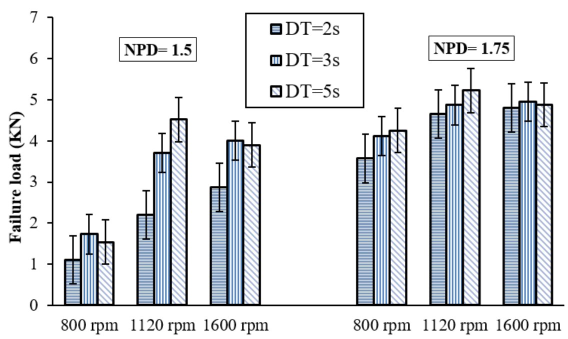

Fig. 6 The effect of normal plunge depth on failure load of friction stir spot welding specimens.

Examination of the plunge depth variations showed that the failure load of the specimens increased as the plunge depth was increased from 1.5 mm to 1.75 mm. The minimum failure load of 1.10 KN was obtained for the specimen prepared at NPD=1.5mm (the minimum NPD); DT=2s; and RS=800rpm. On the other hand, the maximum failure load of 5.23KN was obtained for the specimen prepared at NPD=1.75mm (the maximum NPD); DT=5s; and RS=1120rpm.
Figure 7 shows the effect of NPD on failure load of welded joints. This Figure shows the failure load increased from 2.84 KN to 4.61 KN by increasing the NPD. In other words, increasing the NPD by 16% (from 1.5 mm to 1.75 mm) led to a 1.62-time increase in the failure load. By increasing the NPD, it is obvious that the tool penetration increased. Therefore, the deformed area would expand which in turn generates a larger volume of homogeneous fine-grained material in the stir zone. This occurrence led to an improvement of spot weld s failure load. Whereas increasing the NPD beyond 1.75 mm caused to decrease of the joint failure load. The debilitating happened owing to the fact that the joint thickness diminished due to the high pressure that was applied to the centre of welding region. Then the stirred material stuck out from the welding joint and the failure load decreased drastically because of welding section reduction.

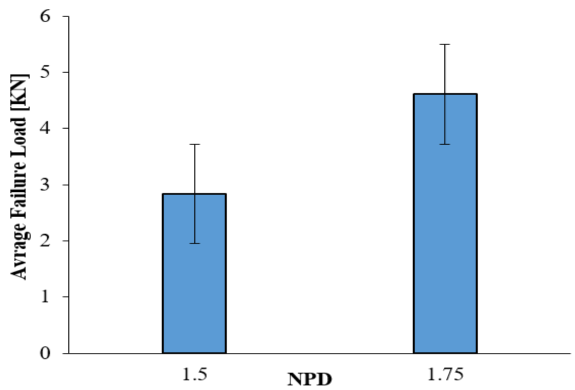

Fig. 7 The effect of normal plunge depth on failure load of friction stir spot welding.

3.2. Effect of Tool Rotational Speed on Failure Load

At a tool rotational speed of 800 rpm, lower joints failure load was consistently observed compared to the rotational speeds of 1120 rpm and 1600 rpm. This decrease in the joints failure load can be attributed to the inadequate material flow that need higher temperature and it caused to lower plastic deformation and also lower dynamic recrystallization.
As shown in "Fig. 8", the failure load increased with a high rate slope by increasing tool rotational speed from 800 rpm to 1120 rpm, and then remained almost constant thereafter 1120 rpm. According to the results, the failure load of the spot-welded joints has increased by about 52% at the first range (from 800 rpm to 1120 rpm). Further increase of rotational speeds to 1600 rpm resulted in production of excessive heat in the welding area, in which the area experienced higher temperatures and also appearance of coarse-grained sediments in that area, which stopped further increase in the welded joint failure load.

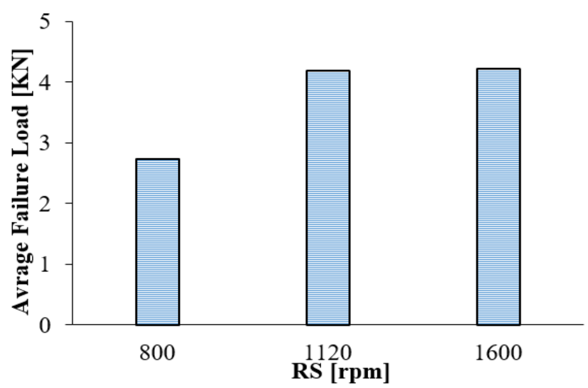

Fig. 8 The effect of rotational speed (RS) on failure load of friction stir spot welding specimens.

3.3. Effect of Dwell Time on Failure Load

As can be seen in "Fig. 9" , the failure load increased with the dwell time in all the tested tool specimens. As the dwell time increased from 2s to 3s, the failure load increased initially at a faster rate (high rate slope) from 3.23 KN to 3.8 KN. Further increase of the dwell time to 5s led to a mean failure load of spot welds increase to 4.05 KN. In other words, the mean failure load experienced an increase of 17% and 6% as the dwell time varied from 2s to 3s and from 3s to 5s, respectively. Grain coarsening at higher welding temperature could be responsible for stopping further increase of the joint failure load.

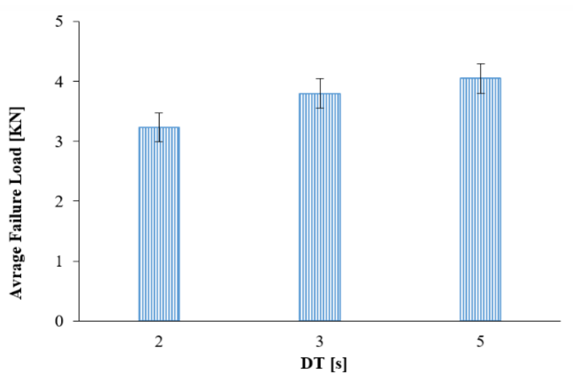

Fig. 9 The effect of dwell time (DT) on failure load of friction stir spot welding specimens.

3.4. Interaction Effects of Welding Process Parameters

In this section, the interaction effects between the FSSW process parameters were investigated. Figure 10 shows the joint failure load versus tool rotational speed.

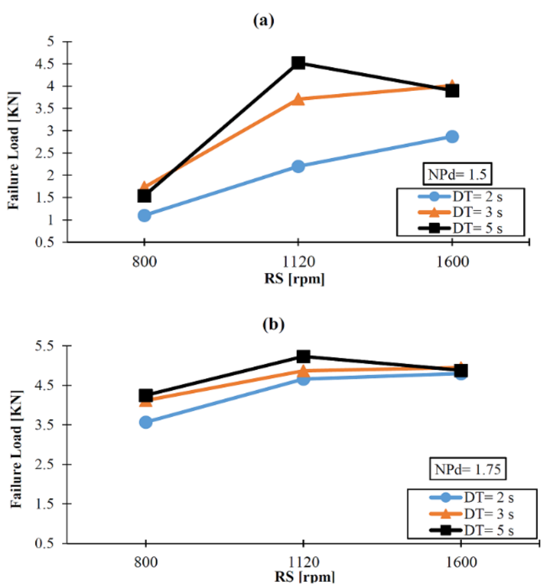

Fig. 10 The effect of rotational speed (RS) on failure load of friction stir spot welding specimens in constant normal plunge depth: (a): 1.5, and (b): 1.75.

As shown, no increase was detected in the failure load upon increasing the rotational speed to 1600 rpm due to the interaction effect with the dwell time. Prolonged dwell time was combined with an excessive increase in rotational speed in which it leads to a drastic increase of temperature especially in welding region. This in turn increases the probability of process defects, increases the volume of coarse-grained materials, reduces dislocations, and possibly deterioration of sediments within the welding area which consequently reduces the failure load. Figure 11 shows the failure load versus tool rotational speed at plunge depths of 1.5 and 1.75 mm. As can be observed, the interaction effects between the rotational speed and plunge depth gradually increase with increasing the tool dwell time.

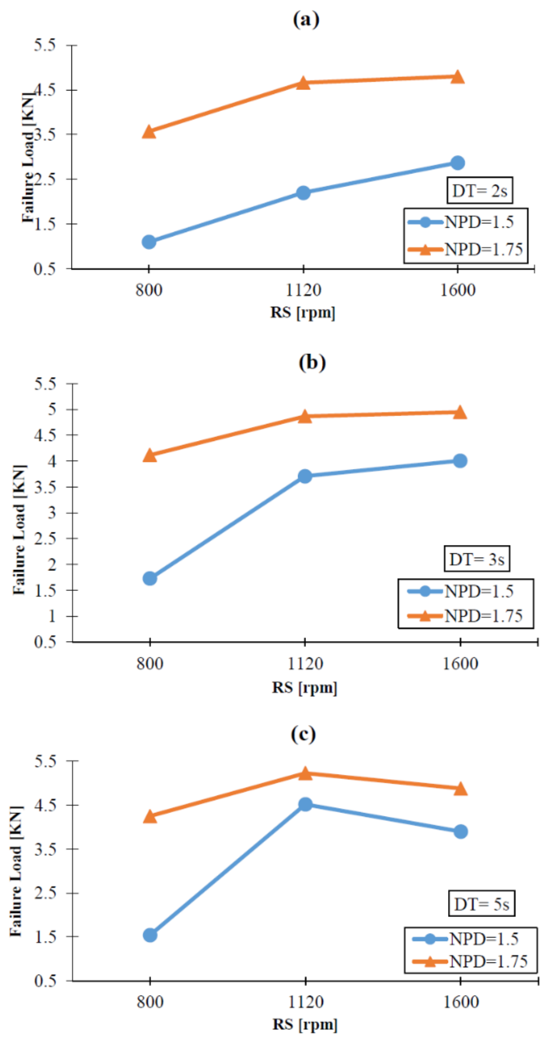

Fig. 11 The effect of rotational speed(RS) on failure load of friction stir spot welding specimens in constant dwell time: (a): 2s, (b): 3s, and (c): 5s.

As can be seen in "Fig. 11" , at dwell time of 2s, interaction effect between the RS and NPD was not observed. At higher dwell time, the interaction effect of NDP and RS increased. Larger NPD of 1.75 with higher dwell time 5s can provide the required welding heat input at tool rotation speed of 800 rpm which significantly increased the joint failure load.

4 CONCLUSION

An experimental study was conducted on the FSSW applied to 2024 T3 aluminium alloy specimens to examine the effects of process parameters (NPD, RS, and DT) on the failure load. The following results were obtained:

1. Increasing the NPD from 1.5 mm to 1.75 mm resulted in a 1.62-time increase in the mean failure load of the spot-welded joints.
2. A 52% increase was observed in the mean failure load by increasing the tool rotational speed from 800 rpm to 1120 rpm. Further increase of rotational speed from 1120 rpm to 1600 rpm did not produce a significant change in the failure load of the specimens.
3. Increasing the tool dwell time from 2s to 3s and from 3s to 5s increased the mean failure load by 17% and 6%, respectively.
4. At higher dwell time, the interaction between the NPD and RS was increased.
5. The highest failure load was obtained for the prepared specimen at RS=1120 rpm; DT=5s; and NPD=1.75mm.

ACKNOWLEDGMENTS

This study was financially supported by The Welding and Non Destructive Testing Applied Research Centre (TWN), University of Tehran. Additionally, the preparation of specimens and mechanical testing equipment were supplied by TWN.

REFERENCES

[1] Daliri, O., Farahani, M., and Farhang, M., A Combined Numerical and Statistical Analysis for Prediction of Critical Buckling Load Of the Cylindrical Shell with Rectangular Cutout, Engineering Solid Mechanics, Vol. 7, 2019, pp. 35-46.

[2] Sam Daliri, O., Farahani, M., Characterization of Stress Concentration in Thin Cylindrical Shells with Rectangular Cutout Under Axial Pressure, International Journal of Advanced Design and Manufacturing Technology, Vol. 10, 2017, pp. 133-141.

[3] Stetco, C., Sam-Daliri, O., Faller, L. M., and Zangl, H., Piezocapacitive Sensing for Structural Health Monitoring in Adhesive Joints, in 2019 IEEE International Instrumentation and Measurement Technology Conference (I2MTC), 2019, pp. 1-5.

[4] Nguyen, N., Kim, D., and Kim, H., Assessment of the Failure Load for an AA6061-T6 Friction Stir Spot Welding Joint, Proceedings of the Institution of Mechanical Engineers, Part B: Journal of Engineering Manufacture, Vol. 225, 2011, pp. 1746-1756.

[5] Farhang, M., Sam-Daliri, O., Farahani, M., and Vatani, A., Effect of Friction Stir Welding Parameters On the Residual Stress Distribution of Al-2024-T6 Alloy, Journal of Mechanical Engineering and Sciences, Vol. 15, 2021, pp. 7684-7694.

[6] Majid, F., Mohammadreza, F., and Mohammad, N., Incorporation of Al2O3 Powder for Improvement of the Mechanical and Metallurgical Properties of Multi-Passes Friction Stir Welding of Al 2024, Iranian Journal of Manufacturing Engineering, Vol. 8, 2021, pp. 35-46.

[7] Shahmirzaloo, A., Farahani, M., and Farhang, M., Evaluation of Local Constitutive Properties of Al2024 Friction Stir-Welded Joints Using Digital Image Correlation Method, The Journal of Strain Analysis for Engineering Design, 2020, pp. 0309324720981201.

[8] Sattari-Far, I. A., Farahani, M., Effect of the Weld Groove Shape and Pass Number On Residual Stresses in Butt-Welded Pipes, International Journal of Pressure Vessels and Piping, Vol. 86, 2009, pp. 723-731.

[9] Ebrahimi, S., Farahani, M., and Akbari, D., The Influences of the Cyclic Force Magnitude and Frequency On the Effectiveness of the Vibratory Stress Relief Process On a Butt Welded Connection, The International Journal of Advanced Manufacturing Technology, Vol. 102, 2019, pp. 2147-2158.

[10] Zamanpour, A., Farahani, M., Farhang, M., and Vafa, N., Experimental Study on the Effects of Harmonic Vibration on the Stress Relief of the Butt Welded AISI 1021 Pipes, 2020.

[11] Pan, T. Y., Friction Stir Spot Welding (FSSW)-a Literature Review, 2007.

[12] Rouzbehani, R., Kokabi, A., Sabet, H., Paidar, M., and Ojo, O., Metallurgical and Mechanical Properties of Underwater Friction Stir Welds of Al7075 Aluminum Alloy, Journal of Materials Processing Technology, Vol. 262, 2018, pp. 239-256.

[13] Saeidi, M., Manafi, B., Besharati Givi, M., and Faraji, G., Mathematical Modeling and Optimization of Friction Stir Welding Process Parameters in Aa5083 and Aa7075 Aluminum Alloy Joints, Proceedings of the Institution of Mechanical Engineers, Part B: Journal of Engineering Manufacture, Vol. 230, 2016, pp. 1284-1294.

[14] Tabasi, M., Farahani, M., Givi, M. B., Farzami, M., and Moharami, A., Dissimilar Friction Stir Welding of 7075 Aluminum Alloy to AZ31 Magnesium Alloy Using SiC Nanoparticles, The International Journal of Advanced Manufacturing Technology, Vol. 86, 2016, pp. 705-715.

[15] Hirasawa, S., Badarinarayan, H., Okamoto, K., Tomimura, T., and Kawanami, T., Analysis of Effect of Tool Geometry On Plastic Flow During Friction Stir Spot Welding Using Particle Method, Journal of Materials Processing Technology, Vol. 210, 2010, pp. 1455-1463.

[16] Badarinarayan, H., Yang, Q., and Zhu, S., Effect of Tool Geometry On Static Strength of Friction Stir Spot-Welded Aluminum Alloy, International Journal of Machine Tools and Manufacture, Vol. 49, 2009, pp. 142-148.

[17] Enami, M., Farahani, M., and Farhang, M., Novel Study On Keyhole Less Friction Stir Spot Welding of Al 2024 Reinforced with Alumina Nanopowder, The International Journal of Advanced Manufacturing Technology, Vol. 101, 2019, pp. 3093-3106.

[18] Karthikeyan, R., Balasubramanian, V., Predictions of the Optimized Friction Stir Spot Welding Process Parameters for Joining AA2024 Aluminum Alloy Using RSM, The International Journal of Advanced Manufacturing Technology, Vol. 51, 2010, pp. 173-183.

[19] Arul, S., Miller, S., Kruger, G., Pan, T. Y., Mallick, P., and Shih, A., Experimental Study of Joint Performance in Spot Friction Welding of 6111-T4 Aluminium Alloy, Science and Technology of Welding and Joining, vol. 13, 2008, pp. 629-637.

[20] Cox, C. D., Gibson, B. T., Strauss, A. M., and Cook, G. E., Effect of Pin Length and Rotation Rate On the Tensile Strength of a Friction Stir Spot-Welded Al Alloy: A Contribution to Automated Production, Materials and Manufacturing Processes, Vol. 27, 2012, pp. 472-478.

[21] Shen, Z., Yang, X., Zhang, Z., Cui, L., and Li, T., Microstructure and Failure Mechanisms of Refill Friction Stir Spot Welded 7075-T6 Aluminum Alloy Joints, Materials & design, Vol. 44, 2013, pp. 476-486.

[22] Mubiayi, M. P., Akinlabi, E. T., An Overview on Friction Stir Spot Welding of Dissimilar Materials, in Transactions on Engineering Technologies, ed: Springer, 2015, pp. 537-549.

[23] Mahoney, M. W., Mishra, R. S., Friction Stir Welding and Processing: ASM International, 2007.

[24] Dolatkhah, A., Golbabaei, P., Givi, M. B., and Molaiekiya, F., Investigating Effects of Process Parameters On Microstructural and Mechanical Properties of Al5052/SiC Metal Matrix Composite Fabricated via Friction Stir Processing, Materials & Design, Vol. 37, 2012, pp. 458-464.

[25] Jamalian, H. M., Farahani, M., Givi, M. B., and Vafaei, M. A., Study on the Effects of Friction Stir Welding Process Parameters On the Microstructure and Mechanical Properties of 5086-H34 Aluminum Welded Joints, The International Journal of Advanced Manufacturing Technology, Vol. 83, 2016, pp. 611-621.

[26] Nazari, M., Besharati Givi, M. K., Farahani, M. R., Mollaei Milani, J., and Mohammad Zadeh, H., Investigation on the Effects of Using Nano-Size Al2O3 Powder On the Mechanical and Microstructural in The Multi-Passes Continuous Friction Stir Welding of the 2024-T6, Modares Mechanical Engineering, Vol. 14, 2015, pp. 85-90.

[27] Bilici, M. K., Yükler, A. I., Influence of Tool Geometry and Process Parameters On Macrostructure and Static Strength in Friction Stir Spot Welded Polyethylene Sheets, Materials & Design, Vol. 33, 2012, pp. 145-152.

[28] Tozaki, Y., Uematsu, Y., and Tokaji, K., Effect of Processing Parameters On Static Strength of Dissimilar Friction Stir Spot Welds Between Different Aluminium Alloys, Fatigue & Fracture of Engineering Materials & Structures, Vol. 30, 2007, pp. 143-148.

[29] Venukumar, S., Yalagi, S., and Muthukumaran, S., Comparison of Microstructure and Mechanical Properties of Conventional and Refilled Friction Stir Spot Welds in AA 6061-T6 Using Filler Plate, Transactions of Nonferrous Metals Society of China, Vol. 23, 2013, pp. 2833-2842.

[30] Bakavos, D., Prangnell, P., Effect of Reduced or Zero Pin Length and Anvil Insulation On Friction Stir Spot Welding Thin Gauge 6111 Automotive Sheet, Science and Technology of Welding and Joining, Vol. 14, 2009, pp. 443-456.

[31] Andalib, H., Farahani, M., and Enami, M., Study on the New Friction Stir Spot Weld Joint Reinforcement Technique on 5754 Aluminum Alloy, Proceedings of the Institution of Mechanical Engineers, Part C: Journal of Mechanical Engineering Science, Vol. 232, 2018, pp. 2976-2986.

[32] Farzami, M., Farahani, M., Akbari, D., and Tabasi, M., "Friction stir weld of AZ91 magnesium alloy with and without nano-SiC particle," JOM, vol. 71, 2019, pp. 4171-4179.

[33] Shahani, A. R., Farrahi, A., Effect of Sheet Thickness on Fatigue Behavior of Friction Stir Spot Weld of Al 6061-T6 Lap-Shear Configuration, Journal of Stress Analysis, Vol. 3, 2018, pp. 61-68.

[34] Hajideh, M. R., Farahani, M., Alavi, S. A. D., and Ramezani, N. M., Investigation on The Effects of Tool Geometry On the Microstructure and The Mechanical Properties of Dissimilar Friction Stir Welded Polyethylene and Polypropylene Sheets, Journal of Manufacturing Processes, Vol. 26, 2017, pp. 269-279.

[35] Badarinarayan, H., Shi, Y., Li, X., and Okamoto, K., Effect of Tool Geometry On Hook Formation and Static Strength of Friction Stir Spot Welded Aluminum 5754-O Sheets, International Journal of Machine Tools and Manufacture, Vol. 49, 2009, pp. 814-823.

[36] Sun, Y., Fujii, H., Takaki, N., and Okitsu, Y., Microstructure and Mechanical Properties of Mild Steel Joints Prepared by A Flat Friction Stir Spot Welding Technique, Materials & Design, Vol. 37, 2012, pp. 384-392.

[37] Rao, H., Jordon, J., Barkey, M., Guo, Y., Su, X., and Badarinarayan, H., Influence of Structural Integrity On Fatigue Behavior of Friction Stir Spot Welded AZ31 Mg Alloy, Materials Science and Engineering: A, Vol. 564, 2013, pp. 369-380.